

Design of a Bimetallic Au/Ag System for Dechlorination of Organochlorides: Experimental and Theoretical Evidence for the Role of the Cluster Effect

Leonid V. Romashov,[†] Levon L. Khemchyan,[†] Evgeniy G. Gordeev,[†] Igor O. Koshevoy,^{‡,§} Sergey P. Tunik,^{*,‡} and Valentine P. Ananikov^{*,†,‡}

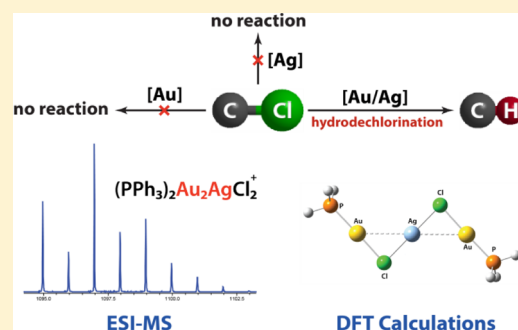
[†]Zelinsky Institute of Organic Chemistry, Russian Academy of Sciences, Leninsky Prosp. 47, Moscow 119991, Russia

[‡]Department of Chemistry, Saint Petersburg State University, Stary Peterhof 198504, Russia

[§]Department of Chemistry, University of Eastern Finland, Joensuu 80101, Finland

Supporting Information

ABSTRACT: The experimental study of dechlorination activity of a Au/Ag bimetallic system has shown formation of a variety of chlorinated bimetallic Au/Ag clusters with well-defined Au:Ag ratios from 1:1 to 4:1. It is the formation of the Au/Ag cluster species that mediated C–Cl bond breakage, since neither Au nor Ag species alone exhibited a comparable activity. The nature of the products and the mechanism of dechlorination were investigated by ESI-MS, GC-MS, NMR, and quantum chemical calculations at the M06/6-311G(d)&SDD level of theory. It was revealed that formation of bimetallic clusters facilitated dechlorination activity due to the thermodynamic factor: C–Cl bond breakage by metal clusters was thermodynamically favored and resulted in the formation of chlorinated bimetallic species. An appropriate Au:Ag ratio for an efficient hydrodechlorination process was determined in a joint experimental and theoretical study carried out in the present work. This mechanistic finding was followed by synthesis of molecular bimetallic clusters, which were successfully involved in the hydrodechlorination of CCl₄ as a low molecular weight environment pollutant and in the dechlorination of dichlorodiphenyltrichloroethane (DDT) as an eco-toxic insecticide. High activity of the designed bimetallic system made it possible to carry out a dechlorination process under mild conditions at room temperature.



INTRODUCTION

Environmental pollution by various chlorinated organic compounds is currently a problem of paramount importance. Various aliphatic and aromatic chlorides have found applications as solvents, dry cleaning fluids, degreasing agents, pesticides, insecticides, etc., and have been produced in large quantities during the last decades. Extensive use and the chemical stability of chlorinated compounds led to critical contamination of the environment by these pollutants.¹ Nowadays, the presence of organochlorides has been detected in ground waters, soils, sediments, algae, plants, animals, and other living organisms. It is important to note that all 12 persistent organic pollutants listed in the “dirty dozen” of the Stockholm Convention are organochlorides.²

Special dechlorination procedures are in demand for conversion of existing pollutants and for the prevention of their further accumulation. Removal of Cl atoms gradually decreases toxicity of chlorinated derivatives; however this is difficult to achieve due to the high stability of organochlorides and the large relative strength of the carbon–chlorine bond. Challenging steps of dechlorination involve breakage of the C–Cl bond, followed by removal of Cl and conversion of the remaining organic part into a less toxic compound.

Existing dechlorination procedures include microbiological dechlorination,³ dechlorination by metals in low oxidation states,⁴ hydrodechlorination,⁵ electrochemical reduction,⁶ and photodegradation.⁷ In recent decades interesting results were achieved using bimetallic compounds as promoters of the dechlorination process. Interaction between different metal atoms may result in superior properties, which significantly exceed a simple combination of individual metals. Various pairs of metals have been studied: Fe–Pd,⁸ Fe–Ni,⁹ Fe–Pt,¹⁰ Fe–Ag,¹¹ Fe–Au,¹¹ Fe–Cu,¹¹ Pd–Au,¹² Pd–Ag,¹³ Pd–Cu,¹³ Pd–Mg,¹⁴ and Pd–Cd.¹⁵ In spite of very promising potential, the origin of the bimetallic effect remains unclear, and a mechanistic picture of bimetallic dechlorination is an intriguing question.

In the present study we have designed a simple *in situ* generated bimetallic Au/Ag system for efficient breakage of the C–Cl bond of chlorinated organic derivatives. A detailed experimental study with electrospray ionization mass spectrometry (ESI-MS) and 1D and 2D NMR spectroscopy and a theoretical study with density functional calculations were

Received: June 11, 2014

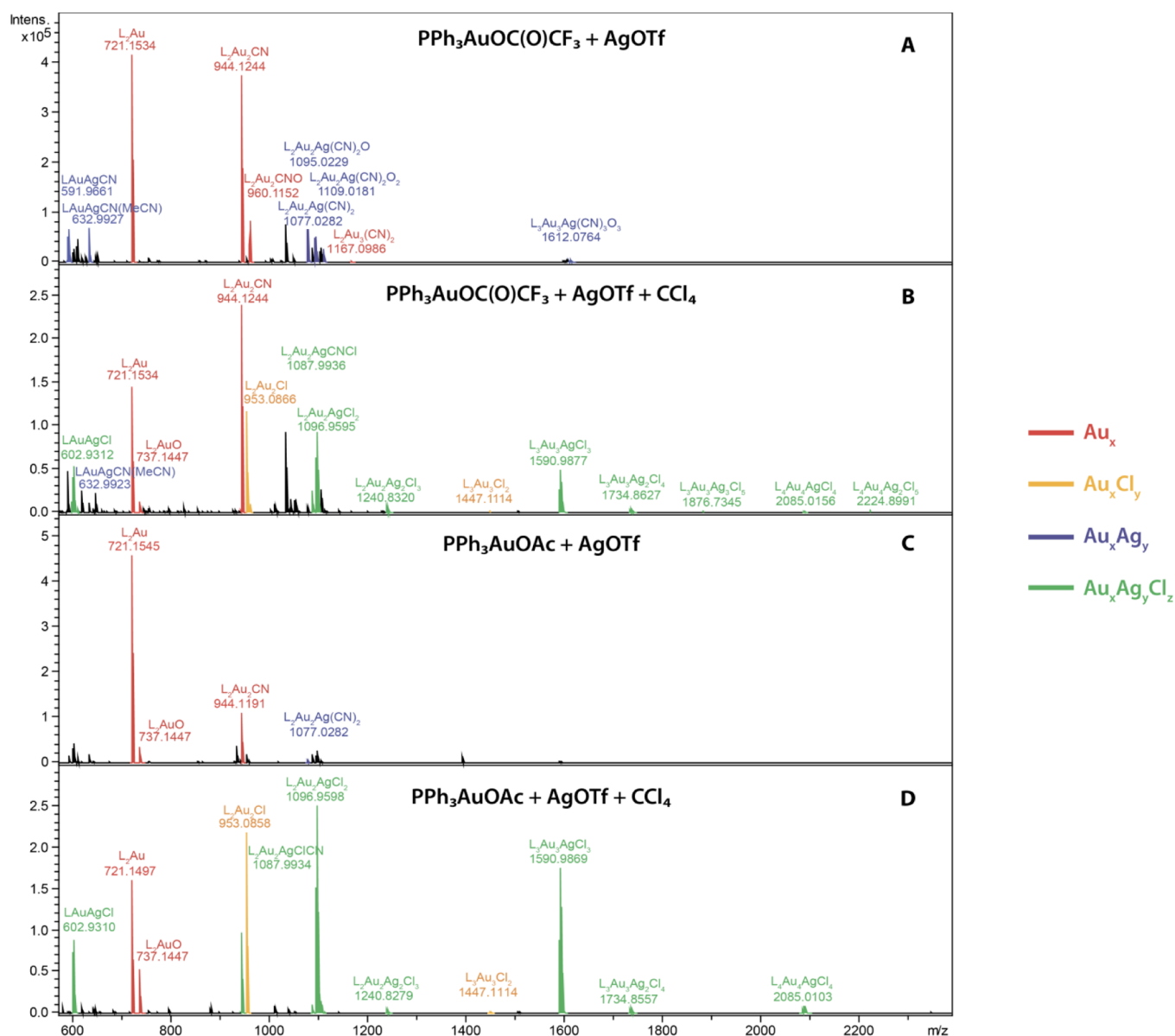


Figure 1. (A) ESI-MS spectrum of the mixture of PPh₃AuOC(O)CF₃ and AgOTf; (B) ESI-MS spectrum of the mixture of PPh₃AuOC(O)CF₃ and AgOTf after reaction with CCl₄; (C) ESI-MS spectrum of the mixture of PPh₃AuOAc and AgOTf; (D) ESI-MS spectrum of the mixture PPh₃AuOAc and AgOTf after reaction with CCl₄ (*i*-PrOH/MeCN solution in all cases); Au-homometallic species are shown in red, chlorinated Au species, in orange; bimetallic Au–Ag species, in violet; and chlorinated bimetallic species, in green (L refers to PPh₃). All shown species are monocations.

carried out to reveal the mechanism of the reaction. The ESI-MS technique was selected for analytical detection of metal clusters as a very informative and powerful tool to study reactions in solution.¹⁶ The optimal Au/Ag combination determined in the mechanistic study was utilized to reveal the key structure of reactive bimetallic clusters. The clusters were prepared in individual form by a separately developed synthetic procedure and successfully applied in the dechlorination of carbon tetrachloride and DDT (1,1,1-trichloro-2,2-bis(4-chlorophenyl)ethane).

RESULTS AND DISCUSSION

Dechlorination with Ag⁺ and Au⁺ Species. As a model reaction we have chosen dechlorination of carbon tetrachloride. CCl₄ is a convenient model molecule containing the desired type of C–Cl functionality. From a practical point of view,

CCl₄ was widely used as a cleaning fluid and degreasing agent. Not surprisingly, CCl₄ is a common pollutant, and its dechlorination is an important problem.

An *i*-PrOH/MeCN mixture was used as reaction media, since it was shown that isopropyl alcohol can be involved as a hydrogen donor during dechlorination¹⁷ and acetonitrile adopts systems to ESI-MS study. In the first step we have evaluated the activity of individual Ag⁺ and Au⁺ species in the dechlorination of CCl₄. For this purpose AgOTf and PPh₃AuOC(O)CF₃ were used as suitable sources of cationic silver and gold species, respectively. Analysis of the registered ESI-MS spectra of both reaction mixtures has shown only traces of chlorinated species (see Supporting Information). Thus, in the individual form neither Ag⁺ nor PPh₃Au⁺ can be considered as an efficient dechlorination agent under the studied conditions.

Superior Bimetallic Effect in Au–Ag-Mediated Dechlorination. The ESI-MS spectrum of the initial Au/Ag mixture prepared by simple dissolution of $\text{PPh}_3\text{AuOC}(\text{O})\text{CF}_3$ and AgOTf showed individual metal species ($(\text{PPh}_3)_2\text{Au}^+$, $(\text{PPh}_3)_2\text{Au}_2\text{CN}^+$, $(\text{PPh}_3)_2\text{Au}_3(\text{CN})_2^+$) as well as bimetallic clusters ($\text{PPh}_3\text{AuAgCN}^+$, $(\text{PPh}_3)_2\text{Au}_2\text{Ag}(\text{CN})_2^+$) (Figure 1A). A combination of PPh_3AuOAc and AgOTf also showed formation of monometallic and bimetallic ions; however, the number of detected species was significantly smaller (Figure 1C). This feature can be explained by the lower electrophilic character of PPh_3AuOAc as compared to $\text{PPh}_3\text{AuOC}(\text{O})\text{CF}_3$.

Remarkably, addition of carbon tetrachloride dramatically changed the composition of the species present in the reaction mixture. In the case of $\text{PPh}_3\text{AuOC}(\text{O})\text{CF}_3$ nearly complete disappearance of halogen-free bimetallic species was observed, and it was accompanied by the appearance of a wide range of chlorinated Au–Ag bimetallic clusters (corresponding signals are shown in green in Figure 1B). At the same time, the signals corresponding to homometallic gold species ($(\text{PPh}_3)_2\text{Au}^+$, $(\text{PPh}_3)_2\text{Au}_2\text{CN}^+$) are preserved after addition of CCl_4 (corresponding signals are shown in red in Figure 1A,B). Thus, the presence of both metals in the cluster was crucial for the C–Cl bond breakage. The appearance of chlorinated species became especially noticeable if PPh_3AuOAc was used as a gold source; signals of chlorinated clusters dominated in the spectrum (Figure 1D). The most intense Cl-containing ions were the same in both experiments: $\text{PPh}_3\text{AuAgCl}^+$, $(\text{PPh}_3)_2\text{Au}_2\text{AgCl}_2^+$, and $(\text{PPh}_3)_3\text{Au}_3\text{AgCl}_3^+$. The corresponding data on the detected signals and composition of related chlorinated bimetallic ions are summarized in Table 1.

Table 1. Composition of Cl-Containing Au–Ag Bimetallic Species Detected in the ESI-MS Spectra of $\text{PPh}_3\text{AuOC}(\text{O})\text{R}/\text{AgOTf}/\text{CCl}_4/i\text{-PrOH}/\text{MeCN}$ Mixtures ($\text{R} = \text{CH}_3, \text{CF}_3$)

no.	m/z	intensity	composition
1	602.93	high	$\text{PPh}_3\text{AuAgCl}$
2	1096.96	high	$(\text{PPh}_3)_2\text{Au}_2\text{AgCl}_2$
3	1240.83	medium	$(\text{PPh}_3)_2\text{Au}_2\text{Ag}_2\text{Cl}_3$
4	1590.99	high	$(\text{PPh}_3)_3\text{Au}_3\text{AgCl}_3$
5	1734.86	medium	$(\text{PPh}_3)_3\text{Au}_3\text{Ag}_2\text{Cl}_4$
6	1876.73	low	$(\text{PPh}_3)_3\text{Au}_3\text{Ag}_3\text{Cl}_5$
7	2085.01	medium	$(\text{PPh}_3)_4\text{Au}_4\text{AgCl}_4$
8	2224.90	low	$(\text{PPh}_3)_4\text{Au}_4\text{Ag}_2\text{Cl}_5$

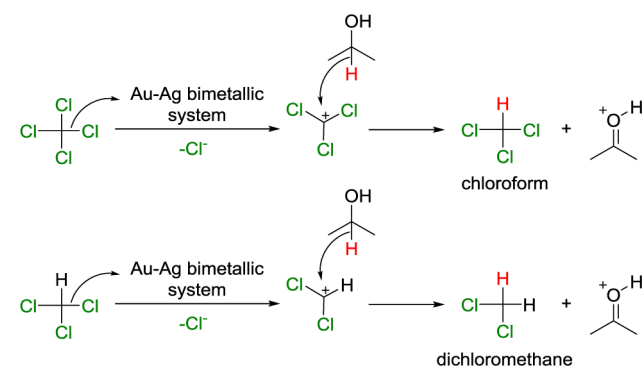
It is important to note that the majority of chlorinated species contained both metals with well-defined Au:Ag ratios from 1:1 to 4:1 (Table 1). Moreover, the signals of chlorinated gold species ($(\text{PPh}_3)_2\text{Au}_2\text{Cl}^+$ and $(\text{PPh}_3)_3\text{Au}_3\text{Cl}_2^+$) were of high intensity in the case of the bimetallic system (Figure 1B,D),

while in the absence of silver salt, formation of halogenated gold species was not observed (see Supporting Information). Thus, silver can be considered a promoter of carbon-to-gold Cl transfer. Indeed, in the observed bimetallic species the detected Cl:Ag ratio in most cases exceeded 1:1. Formation of the complex bimetallic species was observed as a result of a dechlorination reaction, and detected clusters represented the products of this chemical transformation of organochlorides.

The structures of two representative bimetallic cations— $\text{PPh}_3\text{AuAgCl}^+$ and $(\text{PPh}_3)_2\text{Au}_2\text{AgCl}_2^+$ —were probed by means of DFT calculations (Figure 2). In both structures chlorine atoms occupy a bridging position between two metals. The Au–Ag distance decreased upon increasing the number of $\text{H}_3\text{P–Au–Cl}$ fragments connected to silver. This fact can be explained by the amplification of metallophilic interactions during clusterization.¹⁸

^1H , $^{13}\text{C}\{^1\text{H}\}$, and $^1\text{H–}^{13}\text{C}$ HMBC NMR analysis of the reaction mixture demonstrated formation of CH_2Cl_2 in the course of the dechlorination process. Thus, the described reaction can be classified as hydrodechlorination with isopropyl alcohol acting as a hydrogen donor (Scheme 1). Acetone as a

Scheme 1. Proposed Pathway of the Hydrodechlorination Reaction



product of isopropyl alcohol oxidation in the form of its acetal was also detected in the reaction mixture by NMR. Such a procedure involving C–Cl to C–H transformation is of practical importance since it allows easy conversion of chlorinating pollutants into nontoxic products by replacement of Cl atoms with hydrogen.

Revealing the Nature of the Bimetallic Effect by Theoretical Calculations. In order to understand the experimental observations, the mechanism of the studied dechlorination reaction was modeled by means of quantum chemical calculations at the M06/6-311G(d)&SDD level (for more details on the quantum chemical calculations see the Supporting Information). A comparative study involving simple

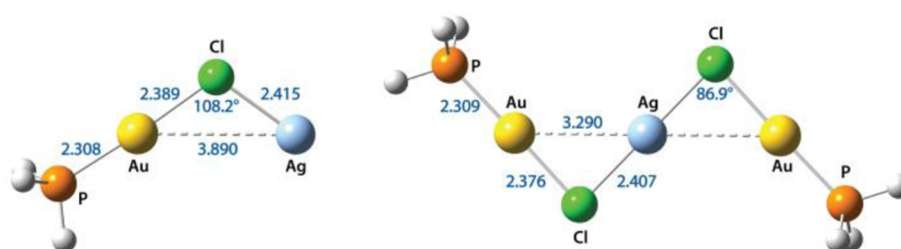
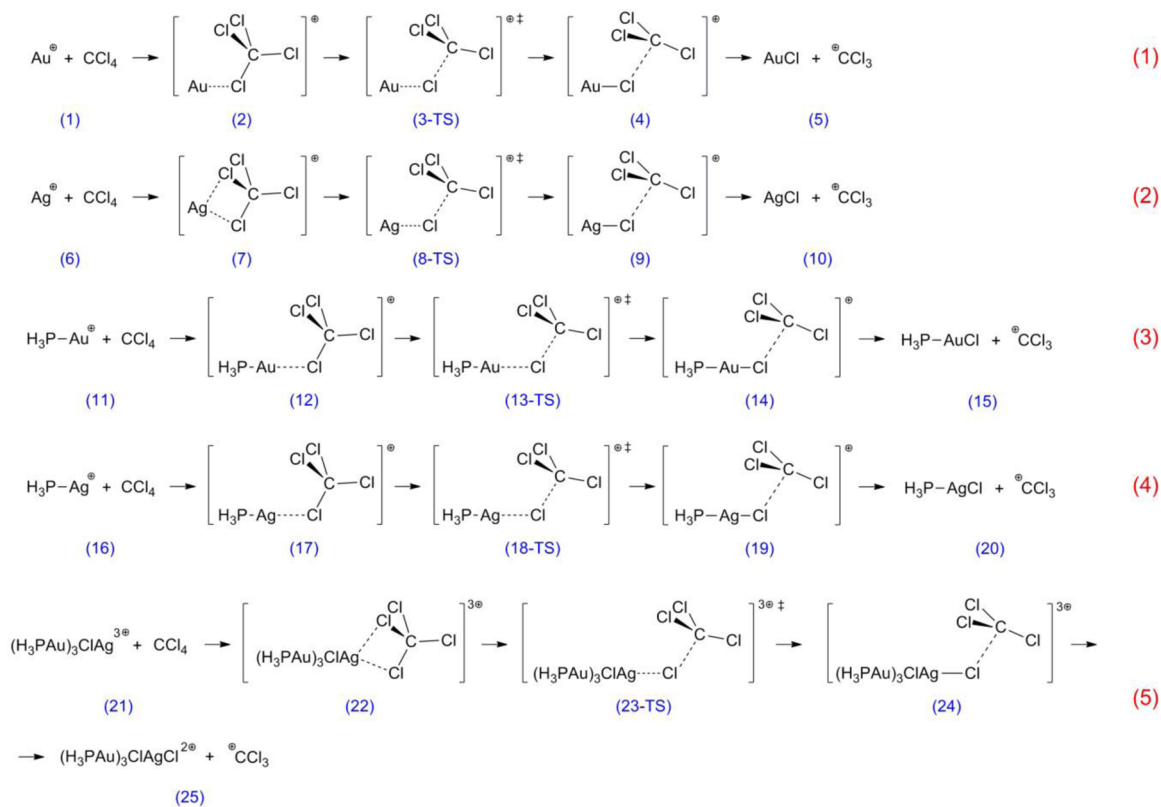


Figure 2. Optimized molecular structures of cations $\text{PH}_3\text{AuClAg}^{(+)}$ (left) and $(\text{PH}_3)_2\text{Au}_2\text{Cl}_2\text{Ag}^{(+)}$ (right) at the M06/6-311G(d)&SDD level.

Scheme 2. Theoretical Study of Metal-Promoted Dechlorination of Carbon Tetrachloride



metal cations (Au^+ and Ag^+), cationic phosphine complexes ($\text{L}-\text{Au}^+$ and $\text{L}-\text{Ag}^+$), and a bimetallic cluster ($\text{L}_3\text{Au}_3\text{Ag}$) was carried out at the same level of theory.

In the first step association of the cation with one or two chlorine atoms of carbon tetrachloride took place (Scheme 2; structures 2, 7, 12, 17, 22) accompanied by significant elongation of the C–Cl bonds participating in the coordination (Figure 3). It should be noted that in the selected model the gold cation coordinated to only one chlorine atom, while the silver cation coordinated to two Cl atoms in the reactions 1 and 5 (Scheme 2).

The transition states of chloride-anion transfer (3-TS, 8-TS, 13-TS, 18-TS, 23-TS) had imaginary frequencies in the range 100–170 cm^{-1} , which corresponded to the transfer of a chloride anion between the carbon and metal centers.¹⁹ In the final step of the process elimination of the $(^+)\text{CCl}_3$ cation took place, leading to formation of the association of this cation with the metal chloride moiety (4, 9, 14, 19, 24). The system with completely separated ions (5, 10, 15, 20, 25) can be considered as the terminal point of the reaction coordinate. Transition states 3-TS, 8-TS, and 23-TS were directly localized by full geometry optimization. Transition states for the metal complexes with a phosphine ligand (13-TS and 18-TS) were not directly localized in the selected model due to the flat energy surface around the TS region. Estimation of the influence of the phosphine ligand on the activation barriers of C–Cl bond breakage was done using constrained geometry optimization.²⁰ Calculation of vibrational spectra for 13-TS and 18-TS confirmed the presence of a single imaginary frequency corresponding to a dechlorination reaction in both cases. Full optimization of structures 14 and 19 did not lead to the planar $(^+)\text{CCl}_3$ cation detached from the metal chloride (in contrast to 4 and 9): the flat cation approached the missing chlorine atom

during optimization and transformed into the reagent. For associates 14 and 19 C–Cl_{Au} and C–Cl_{Ag} distances were fixed at the same values as found for analogous associates 4 and 9, respectively, to estimate the relative energy. The behavior of associates 14 and 19 can be explained by the lower electrophilicity of the metal atom bound to H_3P as compared to the isolated ions $\text{M}^{(+)}$, which is very likely due to electron transfer from the coordinated phosphine ligand.

An analysis of the calculated potential energy surface for the studied reactions (Figure 4) showed that the potential barrier of chloride-anion transfer was rather small in all the cases and changed in the range from 0.7 kcal/mol (for reaction 1) to 8.3 kcal/mol (for reaction 4).

The isolated gold monocation demonstrated a higher affinity to the chloride anion, as compared to the silver cation (reactions 1 and 2; Figure 4). Addition of a phosphine ligand significantly decreased the affinity of the cations to the chloride anion and at the same time increased the energy of all points on the calculated potential energy surface for $\text{H}_3\text{P}-\text{M}^{(+)}$ complexes (reactions 1–4; Figure 4). Thus, variation of ligand environment can be utilized as a tool for tuning the dechlorination activity of the metal cations.

The cationic cluster $(\text{H}_3\text{PAu})_3\text{ClAg}^{(3+)}$ was selected as a model for the study of cluster activity in the dechlorination reaction. The optimized structure of this cluster is depicted in Figure 3 (structure 21). Like in the case of monometallic cations, the dechlorination reaction with 21 started via formation of the starting associate 22, which turned into the product 24 through the transition state 23-TS.

The possibility of structural rearrangements is the key difference between the cluster structure compared to corresponding monometallic cations. This rearrangement happened after addition of a chloride anion from CCl_4 to the

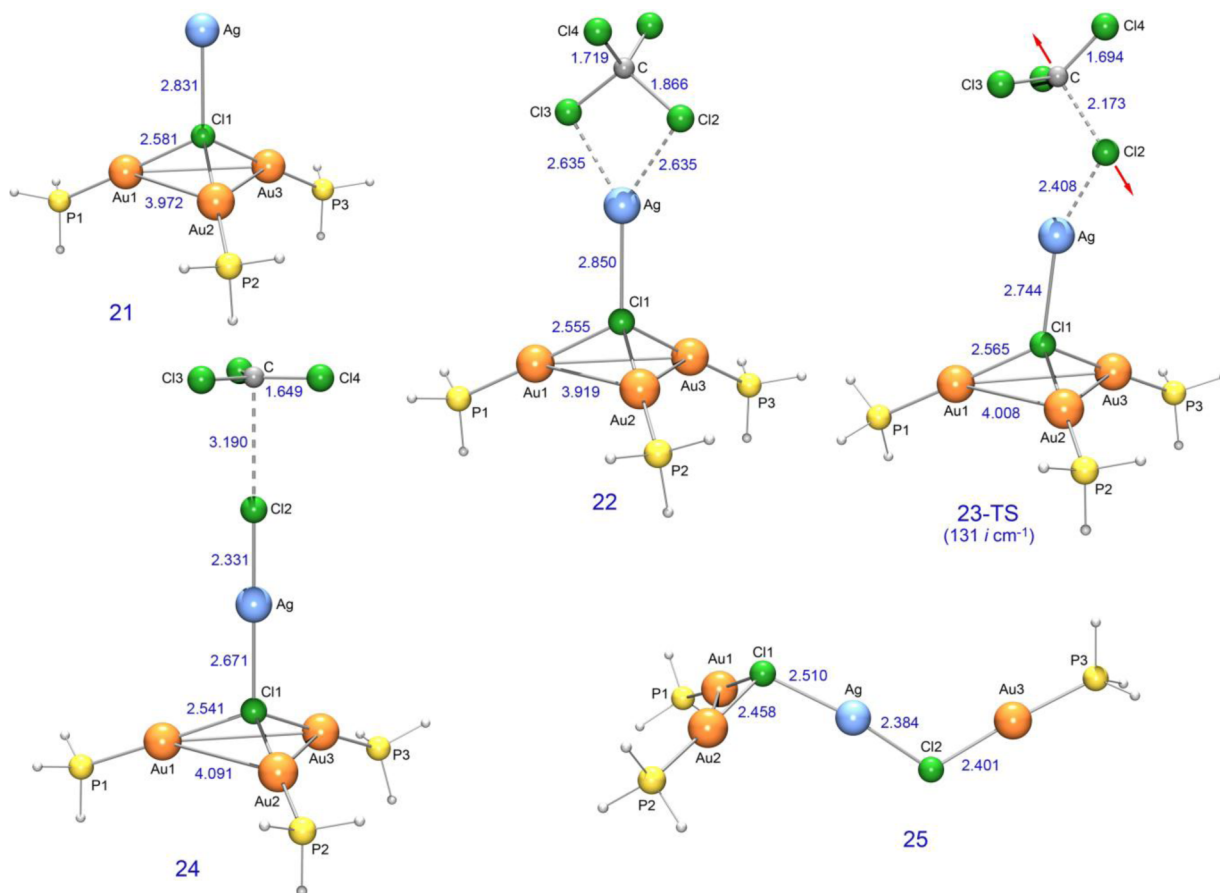


Figure 3. Optimized molecular structures of **21**–**25** for reaction 5 at the M06/6-311G(d)&SDD level (Scheme 2). The normal mode corresponding to imaginary frequency in the transition state is visualized, and interatomic distances are shown in angstroms (see Supporting Information for details).

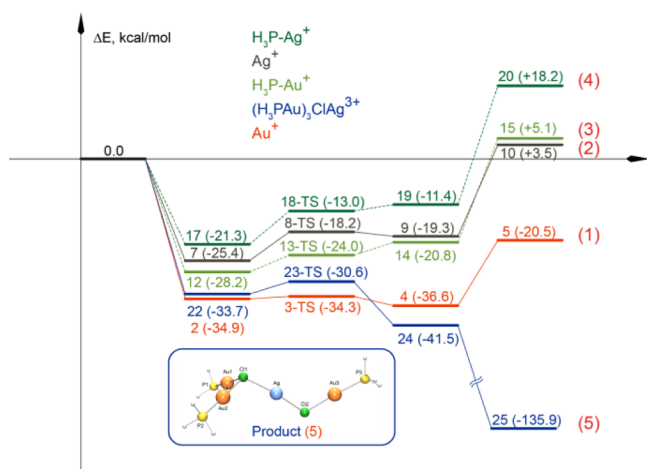


Figure 4. Calculated energy surface (ΔE , kcal/mol) for the carbon tetrachloride dechlorination at the M06/6-311G(d)&SDD level. Each energy surface is marked with the corresponding reaction 1–5 as shown in Scheme 2; color notation is shown for the initial metal species (see Supporting Information for the free energy surface (ΔG) and other details).

cluster cation **24** and led to more efficient binding between the metal and the chlorine atoms, which, in turn, caused a dramatic decrease of product energy (reaction 5; Figure 4). Indeed, the process became highly exothermic (-135.9 kcal/mol) and was favored on the overall potential energy surface. The cluster

effect led to improvement of the dechlorinating activity of the polymetallic cations due to a favorable thermodynamic factor.

On the basis of the analysis of the NBO atomic charge distribution it was shown that structure **24** is characterized by significant change in electron density distribution as compared to structure **25** (see Supporting Information). The studied transition from **24** to **25** was accompanied by a change of the one chlorine atom charge from -0.70 to -0.51 . The charge on the second chlorine atom, remaining in the product **25**, was reduced from -0.53 to -0.47 . The charges of the gold atoms were also reduced, while the charge on the silver atom remained almost unchanged. On this basis, it can be assumed that the transition from **24** to **25** generally leads to a redistribution of electron density and decrease in steric repulsion between positively charged gold atoms, and hence to considerable energy gain.

Cluster Design for Dechlorination. Our experimental and theoretical mechanistic studies have shown that bimetallic Au_2Ag_y clusters exhibited higher activity in dechlorination than monometallic species. ESI-MS measurements indicated that cluster systems with Au_2Ag and Au_3Ag cores are very promising as dechlorinative agents. The ESI-MS-detected clusters were formed *in situ* and were involved in the studied dechlorination process. Unfortunately, such *in situ* formed metal clusters are unisolable and, therefore, are not directly applicable for further practical implementation and process design. At the same time a convenient approach to a variety of stable gold–silver

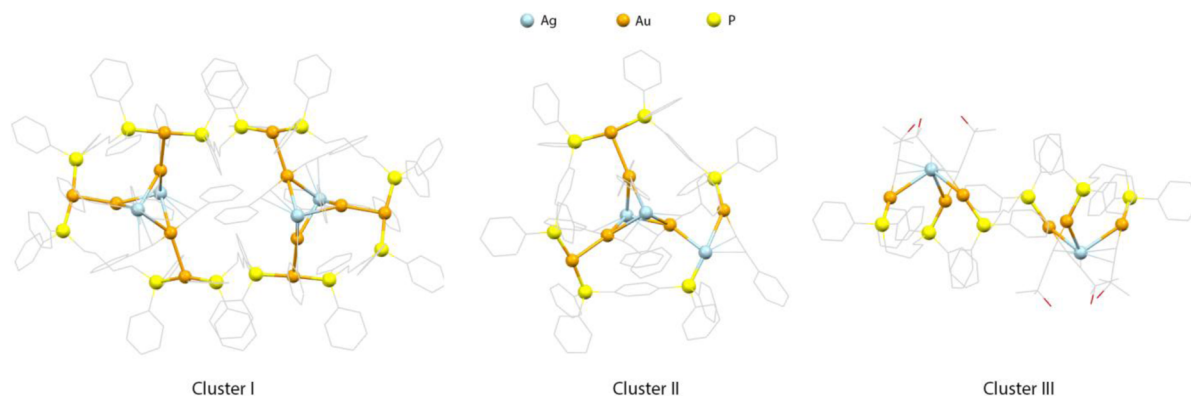
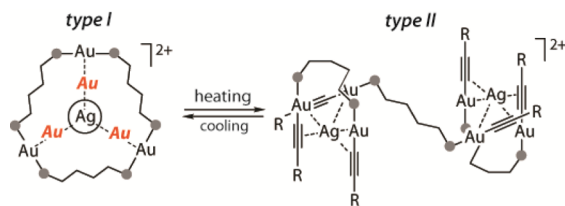


Figure 5. Molecular view of synthesized Au–Ag bimetallic clusters I–III (anions, solvent molecules, and hydrogen atoms are omitted for clarity).

molecular clusters with controlled Au:Ag ratio have been developed (Figure 5).²¹

These heterometallic alkynyl-phosphine complexes can be easily synthesized via self-assembly reactions starting from a gold-alkynyl polymer $[(AuC_2R)_n]$, a silver salt ($AgPF_6$ or $AgClO_4$), and either diphosphine ($Ph_2P-(CH_2)_4-PPh_2$ for I and III) (Figure 5)^{21a} or a simple alkynyl-phosphine gold complex $RC_2Au-P(Ph)_2-C_6H_4-(Ph)_2P-AuC_2R$, II (Figure 5).^{21b} The reactions readily and quickly afforded target complexes with yields higher than 80% after recrystallization of the crude products. It has been shown earlier that the composition and structure of this class of coordination compounds can be determined by geometrical parameters of the diphosphines (the length of the diphosphine spacers) and steric bulkiness of the alkynyl substituents.^{21a,22,23} The general structural motif of these complexes consists of a $\{(Au(C_2R)_2)_3M_2\}$ ($M = Cu, Ag$) central core wrapped by a $\{Au_3(PP)_3\}$ “belt” to form so-called “rods-in-belt” structural patterns.²² In the case of gold–silver complexes one can observe structural variations controlled by the size of the silver ions, which have to be incorporated into the central cluster core. The process results either in opening of the “belt” (complex I)^{21a} or in increasing of the size of the “belt” at the expense of insertion of one more chain-link “Ag– C_2R ” (complex II).^{21b} The complex III was shown to be structurally flexible and existed in solution as an equilibrium mixture of open and closed isomers (Scheme 3).^{21a} In spite of

Scheme 3. Structural Flexibility of Gold–Silver Clusters



the structural differences described above, it can be easily seen that the clusters under study keep the stoichiometry of the major structural fragments ($\{(Au(C_2R)_2)_3Ag_2\}$ or $\{(Au(C_2R)_3)Ag\}$). Independently of the nature of ligands used in the synthesis, the clusters remained stable under various conditions in solution (studied by NMR and ESI-MS) and in the solid state (confirmed by X-ray analysis).^{21a} This clearly points to the inherent stability of these structural units with predetermined Au:Ag ratios. Another consequence of this stability, which is probably even more important, is the

presence of intact metallophilic bonding between silver and gold ions in these structural units, which makes possible a heterometallic effect with participation of Au/Ag clusters in the studied reactions.

In order to prove the concept of cluster effect, the activity of synthesized Au–Ag bimetallic clusters I, II, and III (Figure 5) has been studied in the reaction with carbon tetrachloride.

Analysis of the ESI-MS spectra of cluster I (Figure 6) showed noticeable features similar to the ones described for the above-mentioned system of $PPh_3AuOC(O)R$ and $AgOTf$. Addition of carbon tetrachloride led to (i) nearly complete disappearance of the majority of Au–Ag bimetallic species, which were predominant in the initial spectrum (Figure 6A), and (ii) formation of a variety of chlorinated clusters (Figure 6B).

Amazingly, a common tendency was observed in the behavior of the synthesized ligand-stabilized polynuclear cluster I and Au/Ag species generated *in situ* from monometallic Au and Ag precursors. In both cases chlorinated bimetallic ions were detected upon reaction with CCl_4 under studied conditions (Table 2). Bimetallic Au/Ag ions nearly completely disappear upon addition of CCl_4 . However, there is a significant difference between these two systems. In the case of the *in situ* generated system, formation of the heterometallic core can occur only via assembling around an anionic ligand (Cl^- , Figure 3). Ligand- and alkyne-stabilized clusters (Figure 5) can adopt heterometallic species without any additional stabilization.

Dechlorination of Organochlorides and Cl Removal from DDT. To investigate dechlorinative activity of a Au/Ag bimetallic system on a larger substrate, one of the most “famous” persistent organic pollutants, the insecticide DDT, was involved in the dechlorination reaction under similar conditions. An ESI-MS study was performed to detect metal clusters in solution. Similar Cl-containing ions were observed in the ESI-MS spectrum of the reaction mixture with DDT (Table 2) and CCl_4 (Table 1). Comparison of the ESI-MS spectra showed that for both systems (*in situ* generated and ligand-stabilized clusters) the number of detected chlorine-containing species in DDT dechlorination was smaller than in carbon tetrachloride dechlorination (Tables 1 and 2 and Supporting Information).

For characterization of products, GC-MS analysis of the reaction mixture was carried out and detected formation of two different compounds: (i) 4,4'-(2,2-dichloroethene-1,1-diyl)bis(chlorobenzene), the product of dehydrochlorination of DDT (i.e., removal of HCl); and (ii) 4,4'-(2,2-dichloroethane-1,1-diyl)bis(chlorobenzene), the product of hydrodechlorination of DDT (Cl substitution by H). Indeed, both products can be

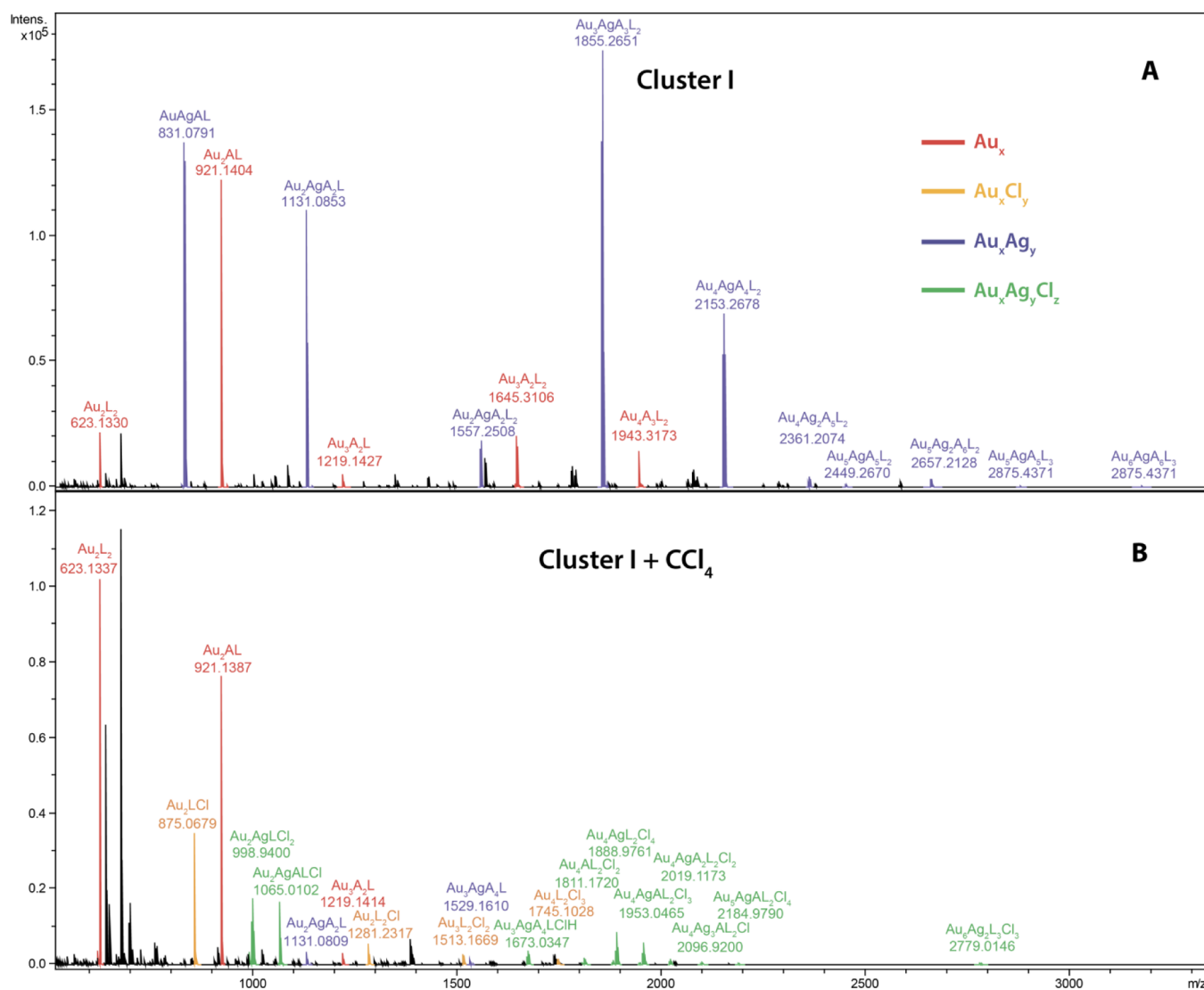


Figure 6. (A) ESI-MS spectrum of cluster I; (B) ESI-MS spectrum of cluster I after reaction with CCl_4 (*i*-PrOH/MeCN solution in all cases); Au-homometallic species are shown in red; chlorinated Au species, in orange; bimetallic Au–Ag species, in violet; and chlorinated bimetallic species, in green (L refers to 1,4-bis(diphenylphosphino)butane, A refers to an alkyne unit, phenylacetylenide). All shown species are monocations.

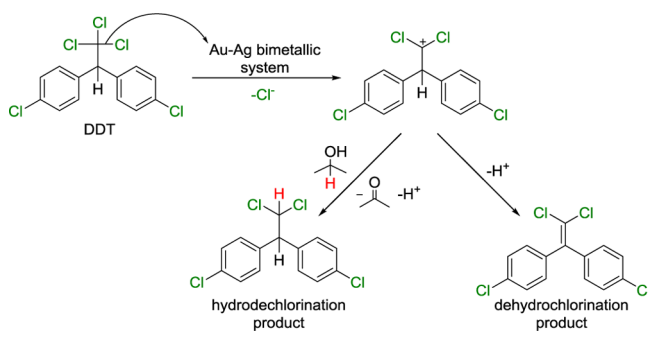
Table 2. Main Chlorinated Metal-Containing Species Detected in the ESI-MS Study of the Dechlorination Reaction (Ligands and Solvent Molecules Are Omitted for Clarity)

metal source	organochloride	detected metallic species
$\text{PPh}_3\text{AuOC}(\text{O})\text{CF}_3$	CCl_4	Au_2Cl (trace)
AgOTf	CCl_4	
$\text{PPh}_3\text{AuOC}(\text{O})\text{CF}_3 + \text{AgOTf}$	CCl_4	AgAuCl , AgAu_2Cl , AgAu_2Cl_2 , AgAu_2Cl_3 , AgAu_2Cl_4 , AgAu_3Cl_3 , $\text{Ag}_2\text{Au}_3\text{Cl}_4$, $\text{Ag}_3\text{Au}_3\text{Cl}_5$, AgAu_4Cl_4 , $\text{Ag}_2\text{Au}_4\text{Cl}_5$, $\text{Au}_2\text{Au}_2\text{Cl}$, Au_3Cl_2
$\text{PPh}_3\text{AuOAc} + \text{AgOTf}$	CCl_4	AgAuCl , AgAu_2Cl , AgAu_2Cl_2 , $\text{Ag}_2\text{Au}_2\text{Cl}_3$, AgAu_3Cl_3 , $\text{Ag}_2\text{Au}_3\text{Cl}_4$, AgAu_4Cl_4 , Au_2Cl , Au_3Cl_2
cluster I	CCl_4	AgAu_2Cl , AgAu_2Cl_2 , AgAu_2 , AgAu_3 , AgAu_3Cl , AgAu_4Cl_4 , AgAu_4Cl_5 , AgAu_4Cl_6 , $\text{Ag}_3\text{Au}_4\text{Cl}_5$, AgAu_5Cl_4 , $\text{Ag}_2\text{Au}_6\text{Cl}_3$, Au_2Cl , Au_3Cl_2 , Au_4Cl_3 , Au_4Cl_2
$\text{PPh}_3\text{AuOAc} + \text{AgOTf}$	DDT	AgAuCl , AgAu_2Cl , AgAu_2Cl_2 , AgAu_3Cl_3 , AgAu_4Cl_4 , Au_2Cl
cluster I	DDT	AuCl , Ag_2Cl , AgAuCl , Ag_2AuCl
cluster II	DDT	
cluster III	DDT	Ag_2Cl , AgAuCl , Au_2Cl

formed after dechlorination of DDT, where the intermediate cation may either eliminate H^+ or subtract hydrogen from isopropyl alcohol (Scheme 4). The process was rendered in a selective manner involving breakage of the aliphatic C–Cl bond in DDT, whereas aromatic C–Cl bonds were not reactive under the studied conditions. The scope of the designed

bimetallic systems was investigated for clusters I, II, and III, and observed metallic species were compared to the bimetallic system accessible *in situ* (Table 2). Formation of polychlorinated species was observed in the case of the *in situ* generated system, while for clusters I and III only monochlorinated species were detected.

Scheme 4. Cl Removal from DDT Using Synthesized Bimetallic Clusters



Cluster I was most active, and cluster III showed moderate activity. Cluster II did not lead to formation of observable metal ions with Cl ligands. Inactivity of cluster II indicates that dynamic behavior in solution (Scheme 3) is not the necessary prerequisite for the reaction.

CONCLUSIONS

A combined experimental and theoretical study was carried out to reveal the nature of the cluster effect in the dechlorination process mediated by a Ag/Au bimetallic system. It was found that most stable chlorinated clusters contained a bimetallic core with a Au:Ag ratio from 1:1 to 4:1. Reaction with CCl_4 occurred via hydrodechlorination, and reduction products were detected by NMR and GC-MS. A theoretical study demonstrated that monometallic silver and gold species were not efficient in C–Cl bond cleavage in carbon tetrachloride, whereas formation of bimetallic clusters improved the dechlorinative activity due to a noticeable thermodynamic factor. The DFT study has indicated highly exothermic structural rearrangement upon formation of chlorinated derivatives of the bimetallic clusters.

As a proof of concept, ligand-stabilized bimetallic Au–Ag clusters have been successfully synthesized and applied in the dechlorination of carbon tetrachloride and DDT. Designed heterometallic systems have shown desired activity in the dechlorination of the C–Cl bond. High activity of the studied bimetallic system made it possible to carry out the dechlorination process under mild conditions at room temperature. Two types of processes for destruction of organochlorides were accessible with the studied bimetallic clusters: hydrodechlorination (CCl_4 and DDT) and dehydrochlorination (DDT).

The experiments have shown the relevance of the studied dechlorination process in the gas phase (*in situ* generated clusters under ESI-MS conditions) and in solution (preformed bimetallic clusters in regular solvent).

EXPERIMENTAL SECTION

General Comments. MeCN (HPLC grade) for ESI-MS experiments was ordered from Merck and used as supplied. Isopropyl alcohol and carbon tetrachloride were distilled and stored over activated 4 Å molecular sieves. The polynuclear heterometallic clusters I, II, and III^{21a} and mononuclear complexes PPh_3AuOAc ,²⁴ $\text{PPh}_3\text{AuOC}(\text{O})\text{CF}_3$,²⁵ and DDT²⁶ were prepared according to the literature procedures. NMR data were collected on a Bruker Avance II 600 spectrometer. GC/MS analyses were performed using a Thermo Scientific Trace GC Ultra equipped with a Thermo TR-5 ms SQC column (15 m × 0.25 mm) and a Thermo MS DSQ II.

Dechlorination Procedure. A 5 mg amount of metal cluster (or a mixture of $\text{PPh}_3\text{AuOC}(\text{O})\text{R}$ and AgOTf), 1 mL of *i*-PrOH, 0.5 mL of MeCN, and 0.5 mL of carbon tetrachloride (or 10 mg of DDT) were placed in an amber glass vial and stirred overnight at room temperature. In the monometallic dechlorination experiments 5 mg of AgOTf or $\text{PPh}_3\text{AuOC}(\text{O})\text{R}$ was used.

Sample Preparation for ESI-MS Analysis. An aliquot (0.04 mL) of the initial solution was dissolved in 1 mL of MeCN, and the obtained solution was diluted 60 times with MeCN and centrifuged for 5 min.

ESI-MS Experiments. High-resolution mass spectra were recorded on a Bruker maXis instrument (Bruker Daltonik GmbH, Bremen, Germany) equipped with an electrospray ionization (ESI) ion source. The measurements were performed in a positive (+MS) ion mode (HV capillary: 4500 V; HV end plate offset: –500 V) with a scan range of m/z 250–10 000. External calibration of the mass spectrometer was performed with electrospray calibrant solution (Fluka). A direct syringe injection was used for the analyzed solutions in MeCN (flow rate: 3 $\mu\text{L}/\text{min}$). Nitrogen was used as nebulizer gas (0.4 bar) and dry gas (4.0 L/min); dry temperature was set at 180 °C. The recorded spectra were processed using the Bruker Data Analysis 4.0 software package.

Theoretical Calculations. The standard 6-311G(d) basis set²⁷ for H, C, Cl, and P and the triple- ζ basis set with the Stuttgart/Dresden effective core potentials²⁸ (SDD) for Ag and Au were used for all calculations (this basis set combination was denoted as 6-311G(d) &SDD). The M06 hybrid density metafunctional²⁹ was applied for geometry optimization and frequency calculations of the reagents, transition states, intermediate complexes, and products. For all calculations a superfine grid was used (Int=SuperFineGrid option). The M06 functional was parametrized for a better description of transition metal atoms²⁹ and should be well suitable for the description of metal clusters.

For all optimized structures the normal coordinate analysis was performed to characterize the nature of the stationary points. Thermodynamic properties of all optimized structures were calculated for 298.15 K and 1 atm. All calculations were carried out using the Gaussian 09 program.³⁰

A suitable guess for the transition states 13-TS and 18-TS was obtained by geometry restraint of Au–Cl1, C–Cl1 (13-TS) and Ag–Cl1, C–Cl1 (18-TS) distances to the same values as obtained for 3-TS and 8-TS, respectively. Both 13-TS and 18-TS had an imaginary frequency corresponding to chloride-anion transfer from the carbon atom to the metal atom.

Molecular structures were visualized by the Ortep III program³¹ and the POV-Ray 3.6 rendering system.³²

ASSOCIATED CONTENT

Supporting Information

Detailed optimized molecular structures, calculated energy surface, calculated energy data for reactions 1–5, NBO calculations, and ESI-MS and NMR data are available free of charge via the Internet at <http://pubs.acs.org>.

AUTHOR INFORMATION

Corresponding Authors

*E-mail (S. P. Tunik): stunik@spbu.ru.

*E-mail (V. P. Ananikov): val@ioc.ac.ru.

Notes

The authors declare no competing financial interest.

ACKNOWLEDGMENTS

This work was supported by the Russian Science Foundation (RNF Grant 14-13-01030) and by RFBR Grants 14-03-31465 and 13-03-12411. The authors also gratefully acknowledge Mr. Gleb D. Rukhovich for help with mass-spectral calculator development.

REFERENCES

- (1) (a) Thornton, J. *Pandora's Poison: Chlorine, Health, and a New Environmental Strategy*; MIT Press: MA, 2000. (b) Loganathan, B. G.; Kannan, K. *Ambio* **1994**, *23*, 187–191. (c) Verreault, J.; Muir, D. C. G.; Norstrom, R. J.; Stirling, I.; Fisk, A. T.; Gabrielsen, G. W.; Derocher, A. E.; Evans, T. J.; Dietz, R.; Sonne, C.; Sandala, G. M.; Gebbink, W.; Riget, F. F.; Born, E. W.; Taylor, M. K.; Nagy, J.; Letcher, R. J. *Sci. Total Environ.* **2005**, *351–352*, 369–390. (d) Roos, A. M.; Bäcklin, B.-M. V. M.; Helander, B. O.; Rigét, F. F.; Eriksson, U. C. *Environ. Pollut.* **2012**, *170*, 268–275.
- (2) The 12 initial persistent organic pollutants (POPs) under the Stockholm Convention. <http://chm.pops.int/TheConvention/ThePOPs/The12InitialPOPs/tabid/296/Default.aspx>.
- (3) (a) Sufliata, J. M.; Horowitz, A.; Shelton, D. R.; Tiedje, J. M. *Science* **1982**, *218*, 1115–1117. (b) Gibson, S. A.; Sufliata, J. M. *Appl. Environ. Microbiol.* **1986**, *52*, 681–688. (c) Krone, U. E.; Laufer, K.; Thauer, R. K.; Hogenkamp, H. P. C. *Biochemistry* **1989**, *28*, 10061–10065. (d) Krone, U. E.; Thauer, R. K.; Hogenkamp, H. P. C. *Biochemistry* **1989**, *28*, 4908–4914. (e) Gantzer, C. J.; Wackett, L. P. *Environ. Sci. Technol.* **1991**, *25*, 715–722. (f) Hardman, D. J. *Crit. Rev. Biotechnol.* **1991**, *11*, 1–40. (g) Scholten, J. D.; Chang, K. H.; Babbitt, P. C.; Charest, H.; Sylvestre, M.; Dunawaymariano, D. *Science* **1991**, *253*, 182–185. (h) Haggblom, M. M. *FEMS Microbiol. Lett.* **1992**, *103*, 29–72. (i) Mohn, W. W.; Tiedje, J. M. *Microbiol. Rev.* **1992**, *56*, 482–507. (j) Raucy, J. L.; Kraner, J. C.; Lasker, J. M. *Crit. Rev. Toxicol.* **1993**, *23*, 1–20. (k) Fetzner, S.; Lingens, F. *Microbiol. Rev.* **1994**, *58*, 641–685. (l) Annachatre, A. P.; Gheewala, S. H. *Biotechnol. Adv.* **1996**, *14*, 35–56. (m) Wilkes, H.; Wittich, R. M.; Timmis, K. N.; Fortnagel, P.; Francke, W. *Appl. Environ. Microbiol.* **1996**, *62*, 367–371. (n) Nagata, Y.; Miyauchi, K.; Damborsky, J.; Manova, K.; Ansorgova, A.; Takagi, M. *Appl. Environ. Microbiol.* **1997**, *63*, 3707–3710. (o) El Fantroussi, S.; Naveau, H.; Agathos, S. N. *Biotechnol. Prog.* **1998**, *14*, 167–188. (p) Fetzner, S. *Appl. Microbiol. Biotechnol.* **1998**, *50*, 633–657. (q) Lee, M. D.; Odom, J. M.; Buchanan, R. J. *Annu. Rev. Microbiol.* **1998**, *52*, 423–452. (r) Häggblom, M. M.; Bossert, I. D. *Dehalogenation: Microbial Processes and Environmental Applications*; Springer: Berlin, 2003; p 520. (s) He, J. Z.; Ritalahti, K. M.; Yang, K. L.; Koenigsberg, S. S.; Löffler, F. E. *Nature* **2003**, *424*, 62–65. (t) Lovley, D. R. *Nat. Rev. Microbiol.* **2003**, *1*, 35–44. (u) Smidt, H.; de Vos, W. M. *Annu. Rev. Microbiol.* **2004**, *58*, 43–73. (v) Borja, J.; Taleon, D. M.; Aurensenia, J.; Gallardo, S. *Process Biochem.* **2005**, *40*, 1999–2013. (w) Schallmeyer, M.; Floor, R. J.; Hauer, B.; Breuer, M.; Jekel, P. A.; Wijma, H. J.; Dijkstra, B. W.; Janssen, D. B. *ChemBioChem* **2013**, *14*, 870–881.
- (4) (a) Gillham, R. W.; Johannesin, S. F. *Ground Water* **1994**, *32*, 958–967. (b) Matheson, L. J.; Tratnyek, P. G. *Environ. Sci. Technol.* **1994**, *28*, 2045–2053. (c) Helland, B. R.; Alvarez, P. J. J.; Schnoor, J. L. *J. Hazard. Mater.* **1995**, *41*, 205–216. (d) Erbs, M.; Hansen, H. C. B.; Olsen, C. E. *Environ. Sci. Technol.* **1999**, *33*, 307–311. (e) Lien, H. L.; Zhang, W. X. *J. Environ. Eng.* **1999**, *125*, 1042–1047. (f) Farrell, J.; Kason, M.; Melitas, N.; Li, T. *Environ. Sci. Technol.* **2000**, *34*, 514–521. (g) Xu, Y.; Zhang, W. X. *Ind. Eng. Chem. Res.* **2000**, *39*, 2238–2244. (h) Lee, W.; Batchelor, B. *Environ. Sci. Technol.* **2002**, *36*, 5147–5154. (i) Elsner, M.; Schwarzenbach, R. P.; Haderlein, S. B. *Environ. Sci. Technol.* **2004**, *38*, 799–807. (j) Quinn, J.; Geiger, C.; Clausen, C.; Brooks, K.; Coon, C.; O'Hara, S.; Krug, T.; Major, D.; Yoon, W. S.; Gavaskar, A.; Holdsworth, T. *Environ. Sci. Technol.* **2005**, *39*, 1309–1318. (k) Li, L.; Fan, M. H.; Brown, R. C.; Van Leeuwen, J. H.; Wang, J. J.; Wang, W. H.; Song, Y. H.; Zhang, P. Y. *Crit. Rev. Environ. Sci. Technol.* **2006**, *36*, 405–431. (l) Zhu, Q. Q.; Mizutani, Y.; Maeno, S.; Fukushima, M. *Molecules* **2013**, *18*, 5360–5372. (m) Roberts, A. L.; Totten, L. A.; Arnold, W. A.; Burris, D. R.; Campbell, T. J. *Environ. Sci. Technol.* **1996**, *30*, 2654–2659. (n) Cantrell, K. J.; Kaplan, D. I.; Wietsma, T. W. *J. Hazard. Mater.* **1995**, *42*, 201–212. (o) Kim, Y. H.; Carraway, E. R. *Environ. Sci. Technol.* **2000**, *34*, 2014–2017. (p) Dries, J.; Bastiaens, L.; Springael, D.; Diels, L.; Combined removal of chlorinated ethenes and heavy metals in zero-valent iron systems. In *Groundwater Quality: Natural and Enhanced Restoration of Groundwater Pollution*; Thornton, S. F.; Oswald, S. E., Eds.; 2002; pp 447–452. (q) Lien, H. L. *Environ. Technol.* **2005**, *26*, 663–672. (r) Song, H.; Carraway, E. R. *Environ. Sci. Technol.* **2005**, *39*, 6237–6245. (s) Li, X. Q.; Elliott, D. W.; Zhang, W. X. *Crit. Rev. Solid State Mater. Sci.* **2006**, *31*, 111–122. (t) Lee, Y. C.; Kim, C. W.; Lee, J. Y.; Shin, H. J.; Yang, J. W. *Desalin. Water Treat.* **2009**, *10*, 33–38. (u) Wang, S. M.; Tseng, S. K. *J. Biosci. Bioeng.* **2009**, *107*, 287–292. (v) Qiu, X. H.; Fang, Z. Q. *Prog. Chem.* **2010**, *22*, 291–297. (w) Wei, Y. T.; Wu, S. C.; Chou, C. M.; Che, C. H.; Tsai, S. M.; Lien, H. L. *Water Res.* **2010**, *44*, 131–140. (x) Comba, S.; Di Molfetta, A.; Sethi, R. *Water, Air, Soil Pollut.* **2011**, *215*, 595–607. (y) Shih, Y. H.; Hsu, C. Y.; Su, Y. F. *Sep. Purif. Technol.* **2011**, *76*, 268–274. (z) Lee, C. L.; Lin, C.; Jou, C. J. *J. Air Waste Manage. Assoc.* **2012**, *62*, 1443–1448.
- (5) (a) Lunin, V. V.; Lokteva, E. S. *Russ. Chem. Bull.* **1996**, *45*, 1519–1534. (b) Simagina, V. I.; Litvak, V. V.; Stoyanova, I. V.; Yakovlev, V. A.; Mastikhin, V. M.; Afanasenkova, I. V.; Likholobov, V. A. *Russ. Chem. Bull.* **1996**, *45*, 1321–1324. (c) Juszczyk, W.; Malinowski, A.; Karpinski, Z. *Appl. Catal., A* **1998**, *166*, 311–319. (d) Scrivanti, A.; Vicentini, B.; Beghetto, V.; Chessa, G.; Matteoli, U. *Inorg. Chem. Commun.* **1998**, *1*, 246–248. (e) Lowry, G. V.; Reinhard, M. *Environ. Sci. Technol.* **1999**, *33*, 1905–1910. (f) Shin, E. J.; Spiller, A.; Tavoularis, G.; Keane, M. A. *Phys. Chem. Chem. Phys.* **1999**, *1*, 3173–3181. (g) Menini, C.; Park, C.; Shin, E. J.; Tavoularis, G.; Keane, M. A. *Catal. Today* **2000**, *62*, 355–366. (h) Yakovlev, V. A.; Terskikh, V. V.; Simagina, V. I.; Likholobov, V. A. *J. Mol. Catal. A: Chem.* **2000**, *153*, 231–236. (i) Choi, Y. H.; Lee, W. Y. *J. Mol. Catal. A: Chem.* **2001**, *174*, 193–204. (j) Zinovyev, S.; Perosa, A.; Yufit, S.; Tundo, P. *J. Catal.* **2002**, *211*, 347–354. (k) Yuan, G.; Keane, M. A. *Catal. Today* **2003**, *88*, 27–36. (l) Yuan, G.; Keane, M. A. *Chem. Eng. Sci.* **2003**, *58*, 257–267. (m) Keane, M. A.; Pina, G.; Tavoularis, G. *Appl. Catal., B* **2004**, *48*, 275–286. (n) Lambert, S.; Polard, J. F.; Pirard, J. P.; Heinrichs, B. *Appl. Catal., B* **2004**, *50*, 127–140. (o) Xia, C. H.; Xu, H.; Wu, W. Z.; Liang, X. M. *Catal. Commun.* **2004**, *5*, 383–386. (p) Yuan, G.; Keane, M. A. *Appl. Catal., B* **2004**, *52*, 301–314. (q) Yuan, G.; Keane, M. A. *J. Catal.* **2004**, *225*, 510–522. (r) Cao, Y. C.; Jiang, X. Z. *J. Mol. Catal. A: Chem.* **2005**, *242*, 119–128. (s) Zinovyev, S. S.; Shinkova, N. A.; Perosa, A.; Tundo, P. *Appl. Catal., B* **2005**, *55*, 39–48. (t) Gryglewicz, S.; Stolarski, M.; Piechocki, W. *Ecol. Chem. Eng.* **2007**, *14*, 77–88. (u) Lokteva, E. S.; Golubina, E. V.; Kachevsky, S. A.; Turakulova, A. O.; Lunin, V. V.; Tundo, P. *Pure Appl. Chem.* **2007**, *79*, 1905–1914. (v) Liu, J. C.; He, F.; Durham, E.; Zhao, D. Y.; Roberts, C. B. *Langmuir* **2008**, *24*, 328–336. (w) He, F.; Liu, J. C.; Roberts, C. B.; Zhao, D. Y. *Ind. Eng. Chem. Res.* **2009**, *48*, 6550–6557. (x) Liu, M. H.; Han, M. F.; Yu, W. W. *Environ. Sci. Technol.* **2009**, *43*, 2519–2524. (y) Lokteva, E. S.; Kachevskii, S. A.; Turakulova, A. O.; Golubina, E. V.; Lunin, V. V.; Ermakov, A. E.; Uimin, M. A.; Mysik, A. A. *Russ. J. Phys. Chem. A* **2009**, *83*, 1300–1306. (z) Fang, Y. L.; Heck, K. N.; Alvarez, P. J. J.; Wong, M. S. *ACS Catal.* **2011**, *1*, 128–138.
- (6) (a) Zhang, S. P.; Rusling, J. F. *Environ. Sci. Technol.* **1993**, *27*, 1375–1380. (b) Fiori, G.; Mussini, P. R.; Rondinini, S.; Vertova, A. *Electrocatalytic Reductive Dehalogenation of Aromatic Halides on Silver*; 2001; Vol. 2001, pp 405–413. (c) Kiflom, W. G.; Wandiga, S. O.; Kamau, G. N. *Pure Appl. Chem.* **2001**, *73*, 1907–1916. (d) Cong, Y. Q.; Wu, Z. C. *Chin. Chem. Lett.* **2007**, *18*, 1013–1016. (e) Durante, C.; Isse, A. A.; Sandona, G.; Gennaro, A. *Appl. Catal., B* **2009**, *88*, 479–489. (f) Durante, C.; Huang, B. B.; Isse, A. A.; Gennaro, A. *Appl. Catal., B* **2012**, *126*, 355–362. (g) Huang, B. B.; Isse, A. A.; Durante, C.; Wei, C. H.; Gennaro, A. *Electrochim. Acta* **2012**, *70*, 50–61. (h) Isse, A. A.; Huang, B. B.; Durante, C.; Gennaro, A. *Appl. Catal., B* **2012**, *126*, 347–354. (i) Durante, C.; Isse, A. A.; Gennaro, A. *J. Appl. Electrochem.* **2013**, *43*, 227–235. (j) Kuroboshi, M.; Idei, H.; Hara, N.; Kokui, Y.; Tanaka, H. *Electrochemistry* **2013**, *81*, 359–361. (k) Shao, J. G.; Richards, K.; Rawlins, D.; Han, B. C.; Hansen, C. A. *J. Porphyrins Phthalocyanines* **2013**, *17*, 317–330. (l) Zhang, Y.; Shen, W.; Ou, Z. P.; Zhu, W. H.; Fang, Y. Y.; Kadish, K. M. *Electroanalysis* **2013**, *25*, 1513–1518.
- (7) (a) Mas, D.; Pichat, P.; Guillard, C. *Res. Chem. Intermed.* **1997**, *23*, 275–290. (b) Czaplicka, M. *J. Hazard. Mater.* **2006**, *134*, 45–59. (c) Horikoshi, S.; Tokunaga, A.; Watanabe, N.; Hidaka, H.; Serpone, N. *J. Photochem. Photobiol., A* **2006**, *177*, 129–143. (d) Terashima, Y.; Ozaki, H.; Giri, R. R.; Tano, T.; Nakatsuji, S.; Takamami, R.

- Taniguchi, S. *Water Sci. Technol.* **2006**, *54*, 55–63. (e) Gao, Z. Q.; Yang, S. G.; Sun, C.; Hong, J. *Sep. Purif. Technol.* **2007**, *58*, 24–31. (f) Parshetti, G. K.; Doong, R. A. *Appl. Catal., B* **2010**, *100*, 116–123. (g) Alimoradzadeh, R.; Assadi, A.; Nasser, S.; Mehrasbi, M. R. *Iran. J. Environ. Health Sci. Eng.* **2012**, *9*. (h) Gao, B.; Liu, L. F.; Liu, J. D.; Yang, F. L. *Appl. Catal., B* **2013**, *138*, 62–69. (i) Lu, S. Y.; Wang, Q. L.; Wu, D.; Li, X. D.; Yan, J. H. *Environ. Prog. Sustainable Energy* **2013**, *32*, 458–464.
- (8) (a) Wei, J. J.; Xu, X. H.; Wang, D. H. *J. Environ. Sci. (Beijing, China)* **2004**, *16*, 621–623. (b) Choi, H.; Al-Abed, S. R.; Agarwal, S.; Dionysiou, D. D. *Chem. Mater.* **2008**, *20*, 3649–3655. (c) Lim, T. T.; Zhu, B. W. *Chemosphere* **2008**, *73*, 1471–1477. (d) Wang, X. Y.; Chen, C.; Liu, H. L.; Ma, J. *Water Res.* **2008**, *42*, 4656–4664. (e) Wu, L. F.; Ritchie, S. M. C. *Environ. Prog.* **2008**, *27*, 218–224. (f) Hildebrand, H.; Mackenzie, K.; Kopinke, F. D. *Environ. Sci. Technol.* **2009**, *43*, 3254–3259. (g) Kustov, L. M.; Finashina, E. D.; Shuvalova, E. V.; Tkachenko, O. P.; Kirichenko, O. A. *Environ. Int.* **2011**, *37*, 1044–1052. (h) Xia, Z.; Liu, H. L.; Wang, S.; Meng, Z. H.; Ren, N. Q. *Chem. Eng. J.* **2012**, *200*, 214–223. (i) Xu, J.; Sheng, T. T.; Hu, Y. J.; Baig, S. A.; Lv, X. S.; Xu, X. H. *Chem. Eng. J.* **2013**, *219*, 162–173. (j) Xu, J.; Tang, J.; Baig, S. A.; Lv, X. S.; Xu, X. H. *J. Hazard. Mater.* **2013**, *244*, 628–636. (k) He, F.; Zhao, D. Y. *Environ. Sci. Technol.* **2005**, *39*, 3314–3320.
- (9) (a) Schrick, B.; Blough, J. L.; Jones, A. D.; Mallouk, T. E. *Chem. Mater.* **2002**, *14*, 5140–5147. (b) Xu, J.; Bhattacharyya, D. *Environ. Prog.* **2005**, *24*, 358–366. (c) Chen, J. M.; Gillham, R. W.; Gui, L. J. *Environ. Sci. Health, Part A: Toxic/Hazard. Subst. Environ. Eng.* **2013**, *48*, 48–56.
- (10) Choi, J.; Lee, W. *Environ. Sci. Technol.* **2008**, *42*, 3356–3362.
- (11) O’Loughlin, E. J.; Kemner, K. M.; Burris, D. R. *Environ. Sci. Technol.* **2003**, *37*, 2905–2912.
- (12) (a) Nutt, M. O.; Hughes, J. B.; Wong, M. S. *Environ. Sci. Technol.* **2005**, *39*, 1346–1353. (b) De Corte, S.; Sabbe, T.; Hennebel, T.; Vanhaecke, L.; De Gussem, B.; Verstraete, W.; Boon, N. *Water Res.* **2012**, *46*, 2718–2726. (c) De Corte, S.; Hennebel, T.; Fitts, J. P.; Sabbe, T.; Biznuk, V.; Verschuere, S.; van der Lelie, D.; Verstraete, W.; Boon, N. *Environ. Sci. Technol.* **2011**, *45*, 8506–8513. (d) Wong, M. S.; Alvarez, P. J. J.; Fang, Y. L.; Akcin, N.; Nutt, M. O.; Miller, J. T.; Heck, K. N. *J. Chem. Technol. Biotechnol.* **2009**, *84*, 158–166.
- (13) Lambert, S.; Ferauche, F.; Brasseur, A.; Pirard, J. P.; Heinrichs, B. *Catal. Today* **2005**, *100*, 283–289.
- (14) (a) Ido, A.; Ishihara, S.; Kume, A.; Nakanishi, T.; Monguchi, Y.; Sajiki, H.; Nagase, H. *Chemosphere* **2013**, *90*, 57–64. (b) Devor, R.; Carvalho-Knighton, K.; Aitken, B.; Maloney, P.; Holland, E.; Talalaj, L.; Elsheimer, S.; Clausen, C. A.; Geiger, C. L. *Chemosphere* **2009**, *76*, 761–766. (c) Coutts, J. L.; Devor, R. W.; Aitken, B.; Hampton, M. D.; Quinn, J. W.; Clausen, C. A.; Geiger, C. L. *J. Hazard. Mater.* **2011**, *192*, 1380–1387.
- (15) Kang, R. H.; Ma, J. H.; Liu, X. H.; He, S. M. *Chin. Chem. Lett.* **1999**, *10*, 607–610.
- (16) Kachala, V. V.; Khemchyan, L. L.; Kashin, A. S.; Orlov, N. V.; Grachev, A. A.; Zalesskiy, S. S.; Ananikov, V. P. *Russ. Chem. Rev.* **2013**, *82*, 648–685.
- (17) Bootharaju, M. S.; Deepesh, G. K.; Udayabhaskararao, T.; Pradeep, T. *J. Mater. Chem. A* **2013**, *1*, 611–620.
- (18) Assadollahzadeh, B.; Schwerdtfeger, P. *Chem. Phys. Lett.* **2008**, *462*, 222–228.
- (19) (a) Cardini, G.; Muniz-Miranda, M.; Pagliai, M.; Schettino, V. *Theor. Chem. Acc.* **2007**, *117*, 451–458. (b) Roy, D.; Furtak, T. E. *Phys. Rev. B* **1986**, *34*, 5111–5117.
- (20) The M–Cl and C–Cl distances in the reactive site of transition states 13-TS and 18-TS were fixed to values similar to those obtained for the transition states 3-TS and 8-TS. The structures 13-TS and 18-TS may be used for approximate estimation of activation barriers for reactions with H₃P–Au⁺ and H₃P–Ag⁺ metal species.
- (21) (a) Koshevoy, I. O.; Karttunen, A. J.; Kritchenkou, I. S.; Krupenya, D. V.; Selivanov, S. I.; Melnikov, A. S.; Tunik, S. P.; Haukka, M.; Pakkanen, T. A. *Inorg. Chem.* **2013**, *52*, 3663–3673. (b) Koshevoy, I. O.; Karttunen, A. J.; Tunik, S. P.; Haukka, M.; Selivanov, S. I.; Melnikov, A. S.; Serdobintsev, P. Y.; Pakkanen, T. A. *Organometallics* **2009**, *28*, 1369–1376.
- (22) (a) Koshevoy, I. O.; Karttunen, A. J.; Tunik, S. P.; Haukka, M.; Selivanov, S. I.; Melnikov, A. S.; Serdobintsev, P. Y.; Khodorkovskiy, M. A.; Pakkanen, T. A. *Inorg. Chem.* **2008**, *47*, 9478–9488. (b) Koshevoy, I. O.; Karttunen, A. J.; Shakirova, J. R.; Melnikov, A. S.; Haukka, M.; Tunik, S. P.; Pakkanen, T. A. *Angew. Chem., Int. Ed.* **2010**, *49*, 8864–8866.
- (23) (a) Koshevoy, I. O.; Ostrova, P. V.; Karttunen, A. J.; Melnikov, A. S.; Khodorkovskiy, M. A.; Haukka, M.; Janis, J.; Tunik, S. P.; Pakkanen, T. A. *Dalton Trans.* **2010**, *39*, 9022–9031. (b) Koshevoy, I. O.; Lin, C.-L.; Karttunen, A. J.; Jänis, J.; Haukka, M.; Tunik, S. P.; Chou, P.-T.; Pakkanen, T. A. *Chem.—Eur. J.* **2011**, *17*, 11456–11466. (c) Weber, D.; Jones, T. D.; Adduci, L. L.; Gagné, M. R. *Angew. Chem., Int. Ed.* **2012**, *51*, 2452–2456.
- (24) Preisenberger, M.; Schier, A.; Schmidbaur, H. *J. Chem. Soc., Dalton Trans.* **1999**, 1645–1650.
- (25) Darling, S. F. *J. Chem. Educ.* **1945**, *22*, 170.
- (26) (a) Krishnan, R.; Binkley, J. S.; Seeger, R.; Pople, J. A. *J. Chem. Phys.* **1980**, *72*, 650–654. (b) McLean, A. D.; Chandler, G. S. *J. Chem. Phys.* **1980**, *72*, 5639–5648.
- (27) (a) Schwerdtfeger, P.; Dolg, M.; Schwarz, W. H. E.; Bowmaker, G. A.; Boyd, P. D. W. *J. Chem. Phys.* **1989**, *91*, 1762–1774. (b) Andrae, D.; Häußermann, U.; Dolg, M.; Stoll, H.; Preuß, H. *Theor. Chim. Acta* **1990**, *77*, 123–141. (c) Bergner, A.; Dolg, M.; Küchle, W.; Stoll, H.; Preuß, H. *Mol. Phys.* **1993**, *80*, 1431–1441.
- (28) (a) Zhao, Y.; Truhlar, D. *Theor. Chem. Acc.* **2008**, *120*, 215–241. (b) Zhao, Y.; Truhlar, D. G. *Acc. Chem. Res.* **2008**, *41*, 157–167. (c) Zhao, Y.; Truhlar, D. G. *Chem. Phys. Lett.* **2011**, *502*, 1–13.
- (29) (a) Frisch, M. J.; Trucks, G. W.; Schlegel, H. B.; Scuseria, G. E.; Robb, M. A.; Cheeseman, J. R.; Scalmani, G.; Barone, V.; Mennucci, B.; Petersson, G. A.; Nakatsuji, H.; Caricato, M.; Li, X.; Hratchian, H. P.; Izmaylov, A. F.; Bloino, J.; Zheng, G.; Sonnenberg, J. L.; Hada, M.; Ehara, M.; Toyota, K.; Fukuda, R.; Hasegawa, J.; Ishida, M.; Nakajima, T.; Honda, Y.; Kitao, O.; Nakai, H.; Vreven, T.; Montgomery, J. A., Jr.; Peralta, J. E.; Ogliaro, F.; Bearpark, M.; Heyd, J. J.; Brothers, E.; Kudin, K. N.; Staroverov, V. N.; Kobayashi, R.; Normand, J.; Raghavachari, K.; Rendell, A.; Burant, J. C.; Iyengar, S. S.; Tomasi, J.; Cossi, M.; Rega, N.; Millam, N. J.; Klene, M.; Knox, J. E.; Cross, J. B.; Bakken, V.; Adamo, C.; Jaramillo, J.; Gomperts, R.; Stratmann, R. E.; Yazyev, O.; Austin, A. J.; Cammi, R.; Pomelli, C.; Ochterski, J. W.; Martin, R. L.; Morokuma, K.; Zakrzewski, V. G.; Voth, G. A.; Salvador, P.; Dannenberg, J. J.; Dapprich, S.; Daniels, A. D.; Farkas, Ö.; Foresman, J. B.; Ortiz, J. V.; Cioslowski, J.; Fox, D. J. *Gaussian 09, Revision D.01*; Gaussian, Inc.: Wallingford, CT, 2009.
- (30) Farrugia, L. *J. Appl. Crystallogr.* **2012**, *45*, 849–854.
- (31) Cason, C.; Froehlich, T.; Kopp, N.; Parker, R. *POV-Ray for Windows, V. 3.6.2*; Persistence of Vision Raytracer Pty. Ltd.: 2009.